

# Enhancement of Centrifugal Compressor Operating Range by Use of Inlet Fins

**TAMAKI Hideaki** : Doctor of Engineering, P. E. Jp, Fellow, Corporate Research & Development  
**OOUCHIDA Satoshi** : Turbo Machinery and Engine Technology Department, Products Development Center, Corporate Research & Development  
**UNNO Masaru** : Manager, Numerical Analysis Department, Research Laboratory, Corporate Research & Development  
**TANAKA Ryuuta** : Advanced Technology Department, Research & Engineering Division, Aero-Engine & Space Operations  
**YAMAGUCHI Satoshi** : General Manager, Production Design & Development Division, IHI Turbo Co., Ltd.

The operational points of a turbocharger compressor have a strong tendency to approach its surge conditions (stability limit) during an engine's acceleration period, particularly under low engine-speed conditions. Hence there are expectations for a method for shifting the stability limit on a compressor low-speed line toward a lower flow rate. Inlet recirculation is often observed in a centrifugal compressor with a vaneless diffuser near a surge and under low compressor-speed conditions. The reverse flow caused by the inlet recirculation grows in a compressor-inlet pipe in the upstream direction. Firstly, this paper discusses the effect of inlet recirculation on compressor characteristics by considering a 1-D model and the potential that the growth of inlet recirculation has shown for destabilizing compressor operations. Secondly, the flow in a compressor-inlet pipe of a turbocharger was shown using visualization techniques, namely, oil flow and PIV (Particle Image Velocimetry), confirming the existence of inlet recirculation in the tested compressor. Furthermore, the effect of small fins mounted in a compressor-inlet pipe on inlet recirculation and compressor characteristics under low-speed conditions was investigated. Small fins are called inlet fins in this paper. According to test results, inlet fins showed great promise in shifting the compressor stability limit toward a low flow rate during inlet recirculation.

## 1. Introduction

A turbocharger compressor can be operated in a limited flow rate range. Assuming the turbocharger compressor is operating at a constant rotation speed, the flow rate of the compressor will reach its maximum operational limit when the flow speed in an impeller or diffuser, which are constituent elements of the turbocharger compressor, reaches the speed of sound (choked). In contrast, the flow rate will reach the minimum operational limit when rotating stall or surge (an intensive oscillation phenomenon associated with abnormal sound) is generated.

A smaller engine mounted with a turbocharger significantly improves the fuel efficiency of passenger vehicles.<sup>(1)</sup> The operating point of the centrifugal compressor used in the turbocharger has a tendency to approach its surge region when an engine is accelerating. In contrast, when the engine is operated at maximum power, it requires a correspondingly large flow rate. That is, the centrifugal compressor of a turbocharger is required to reduce the surge flow rate when an impeller is in a low rotation speed range and maintain or increase a choked flow rate when the impeller is in a high rotation speed range. Because it is relatively easy to design a centrifugal compressor that ensures the choked flow rate of the impeller, the technologies for reducing the surge flow rate at a low rotation speed range are the important factors that will

differentiate turbocharging performance from the competitors.

Centrifugal compressors with vaneless diffusers like those used in turbochargers are likely to generate inlet recirculation in the vicinity of the surge. As illustrated in **Fig. 1**, inlet recirculation is a flow phenomenon in which fluid discharged upstream from an impeller inlet flows back to the impeller after merging with a flow of the fluid inside a suction pipe attached to the inlet of a compressor.<sup>(2)</sup> Little experimental research has been done on the inlet recirculation generated in centrifugal compressors. However, the generation of inlet recirculation is frequently encountered (whether it actually exists or not) in the results of steady analysis of a single pitch of an impeller blade using CFD (Computational Fluid Dynamics)

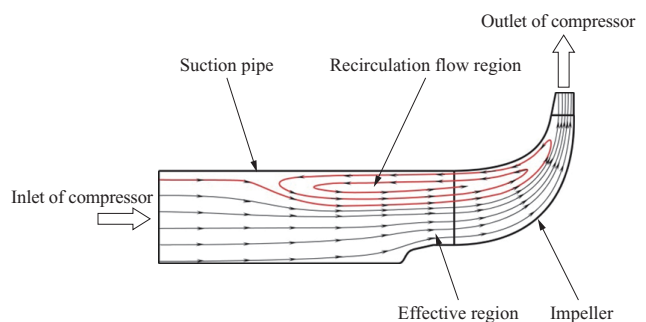


**Fig. 1** Meridional streamline of inlet recirculation<sup>(2)</sup>

which is conducted when designing compressors.<sup>(3)</sup> Harley et al. derived the relationship between the area of a reverse flow section due to inlet recirculation and operating conditions by applying a similar single pitch analysis to various impellers on turbocharger compressors<sup>(4)</sup> and advocated the necessity of improving the loss prediction model for inlet recirculation proposed by Qui et al.<sup>(5)</sup> Anderson et al. conducted experiments to measure the growth of inlet recirculation (reverse flow) generated at the impeller of a turbocharger compressor with thermocouples arranged at positions along several axial directions of the suction pipes of the compressor.<sup>(6)</sup>

As described later, the generation of inlet recirculation has the possibility to make the compressor characteristics (the relationship between pressure ratios and flow rates: a P-Q curve) have a positive gradient. In the region where the compressor characteristics have a positive gradient, a compressor is likely to generate surge and the operation of the compressor without surge is only possible when the flow resistance of a connection pipe and the gradient of the compressor characteristics meet specific conditions. Thus, it is expected that the reduction in surge flow rate can be achieved by controlling the generation and growth of inlet recirculation.

In this research, small-scale fins (hereinafter referred to as “inlet fins”) were installed in the suction pipe of a compressor to control the growth of inlet recirculation. The results showed that the inlet fins successfully reduced the surge flow rate without altering the compressor characteristics in the high rotation speed region. Updated data on the research is reported in the reference (7).

## 2. Symbol

The meanings of the symbols used in this paper are as follows.

- $C_p$  : Constant pressure specific heat (J/kg/K)
- $C_u$  : Speed in a circumferential direction (m/s)
- $C_z$  : Speed in an axial direction (m/s)
- $m$  : Compressor flow rate (kg/s)
- $m_d$  : Reference flow rate (kg/s)
- $M_u$  : Peripheral Mach number ( $= u_2/(\gamma R_g T_0)^{0.5}$ )
- $\gamma$  : Specific heat ratio
- $N$  : Rotational speed (rpm)
- $P$  : Static pressure (Pa)
- $R_g$  : Gas constant (J/kg/K)
- $r$  : Radius (m)
- $T_0$  : Total temperature or total temperature at an inlet of a compressor (K)
- $u_2$  : Peripheral speed ( $= 2\pi r_2 N/60$ ) (m/s)
- $z$  : Position in an axial direction (m)
- $\eta$  : Compressor efficiency
- $\pi$  : Pressure ratio of a compressor (Total to Total) or circular constant
- $\rho$  : (Static) density (kg/m<sup>3</sup>)
- $R$  : Radius at a blade tip (m)
- $c$  : Blade tip clearance (m)
- $C_a$  : Flow speed in an axial direction at blade tip clearance section (m/s)
- $F_w$  : Force acting on fluid at a blade tip clearance from a casing wall (N/m<sup>2</sup>)

- $F_t$  : Force acting on fluid at a blade tip clearance from fluid near a blade tip at a blade side (N/m<sup>2</sup>)
- $k_1$  : Coefficient (equivalent to viscosity coefficient) (Pa·s)
- $C_z$  : Flow speed of fluid around a blade tip in an axial direction at a blade side (m/s)
- $E$  : Work transferred from an impeller blade to fluid (J/kg/s)
- $u$  : Circumferential speed of a blade tip ( $= 2\pi R N/60$ ) (m/s)
- $\omega$  : Angular speed ( $= 2\pi N/60$ ) (rad/s)
- $\beta_{b1}$  : Angle of impeller blade (degree)
- $k_2$  : Proportionality coefficient (-)
- $\Delta E_f$  : Angular momentum of fluid passing through an impeller (kg·m/s<sup>2</sup>)
- $h$  : Specific enthalpy (J/kg)
- Suffix
- 1 : Leading edge of an impeller
- 2 : Outlet of an impeller
- $b$  : Reverse flow

## 3. Discussion on inlet recirculation using 1-D model

In this section, the onset conditions of inlet recirculation are discussed. **Figure 2** shows a schematic diagram of a flow at the section near an impeller blade tip and a gap between the impeller blade tip and casing wall. Now, consider the balance of the momentum at the section in the axial direction. Given  $F_w$  is the force per unit area acting on fluid from a casing wall and  $F_t$  is the fluid at a blade section, the following equation is derived from the law of conservation of momentum:

$$\frac{\partial}{\partial z} (2\pi R c \rho C_a^2) \Delta z = (F_t - F_w) 2\pi R \Delta z - \frac{\partial P}{\partial z} \Delta z 2\pi R c \dots\dots\dots (1)$$

Here,  $(F_t - F_w)$  is considered to be proportional to the difference between a speed component in an axial direction  $C_z$  and a speed on a wall (which is 0 because of no slip conditions on the wall surface) of the fluid near the impeller blade tip (speed gradient). Then,

$$k_1 \frac{C_z}{c} = F_t - F_w \dots\dots\dots (2)$$

Assuming that the change in the radius  $R$  of the impeller blade tip in the axial direction is very small, the following equation can be obtained from equations (1) and (2):

$$\rho \frac{\partial C_a^2}{\partial z} = k_1 \frac{C_z}{c^2} - \frac{\partial P}{\partial z} \dots\dots\dots (3)$$

The conditions under which a reverse flow is generated between the impeller blade tips can be expressed as follows

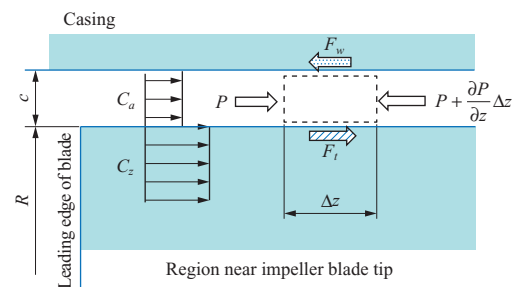


**Fig. 2** Schematic of flow near and between impeller tips

based on the balance of force:

$$0 > k_1 \frac{C_z}{c^2} - \frac{\partial P}{\partial z} \dots\dots\dots (4)$$

Then, the onset criteria (criteria of judgment) can be expressed by:

$$k_1 \frac{C_z}{c^2} - \frac{\partial P}{\partial z} = 0 \dots\dots\dots (5)$$

Focusing on the leading edge of the impeller, given that inlet pre-swirl is 0, the Euler equation (the work transferred from the impeller to the fluid per unit time and unit mass) at the impeller blade tip is

$$\Delta E = uC_u \dots\dots\dots (6)$$

With an angular speed of  $\omega$ , the force  $F$  acting on the fluid flowing through the impeller blade tip per unit mass flow rate can be expressed by

$$F = \frac{\Delta E}{\omega R} = C_u = u - C_z \tan \beta_{b1} \dots\dots\dots (7)$$

Here,  $F$  is proportional to the load on the impeller blade tip (the pressure difference between positive and negative pressure faces). Then, given  $\Delta P_{p-s}$  as the impeller blade load near the leading edge of the impeller blade,

$$F = k_2 \Delta P_{p-s} \dots\dots\dots (8)$$

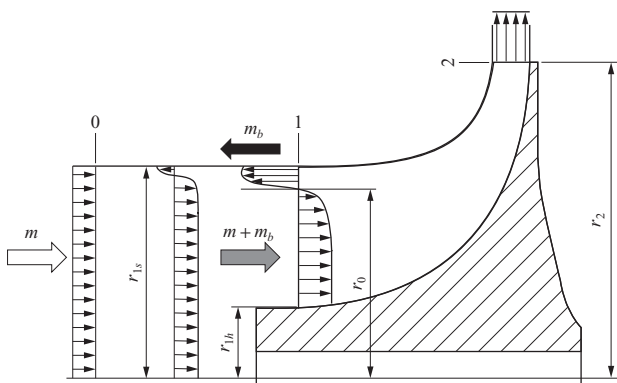
Thus,

$$C_z = \frac{u - k_2 \Delta P_{p-s}}{\tan \beta_{b1}} \dots\dots\dots (9)$$

Equations (5) and (9) show that when the flow rate, which is the speed in the axial direction  $C_z$ , is reduced and the impeller blade load (incidence angle) exceeds a certain value, the adverse pressure gradient generated by the impeller blade itself generates inlet recirculation. Also, equation (4) explains that inlet recirculation can be generated with  $C_z = 0$  when separation occurs at the leading edge of the impeller.

**Figure 3** shows a schematic diagram of the flow around the impeller associated with inlet recirculation.<sup>(7)</sup> The difference in the angular momentum between positions 1 and 2 ( $\Delta L_{1-2}$ ) in **Fig. 3** can be expressed as follows:

$$\Delta L_{1-2} = mr_2 C_{u2} - \left[ \int_{r_{1h}}^{r_0} r C_u (2\pi r \rho C_z) dr + \int_{r_0}^{r_{1s}} r C_u (2\pi r \rho C_z) dr \right] \dots\dots\dots (10)$$



(Note)  $r_{1s}$  : Shroud radius of impeller inlet  
 $r_0$  : Location where speed in the axial direction becomes 0  
 $r_{1h}$  : Radius of impeller hub  
 $r_2$  : Radius of impeller

**Fig. 3** Schematic of flow in impeller with inlet recirculation<sup>(7)</sup>

Where  $r_0$  is the radial location where the speed in the axial direction becomes 0. The work supplied to the fluid by the impeller per unit time  $W$  is:

$$W = \omega \Delta L_{1-2} = (mu_2 C_{u2} - \Delta E_f) + \Delta E_b \dots\dots\dots (11)$$

$$\Delta E_f = \int_{r_{1h}}^{r_0} u C_u (2\pi r \rho C_z) dr \dots\dots\dots (11a)$$

$$\Delta E_b = \int_{r_0}^{r_{1s}} u C_u (2\pi r \rho (-C_z)) dr \dots\dots\dots (11b)$$

Where  $\omega$  is the angular speed of the impeller,  $u$  is the product of radius  $r$  and  $\omega$ ,  $\Delta E_b$  is the work supplied to the fluid flowing from the impeller on the upstream side of the impeller and  $(mu_2 C_{u2} - \Delta E_f)$  is the work applied to the fluid flowing out of the outlet of the impeller. In this formula,  $-\Delta E_f$  means the induction of a swirl in the same direction as the rotational direction of the impeller at the impeller inlet (positive pre-swirl). The following equation can be obtained by applying the law of conservation of angular momentum to a region between positions 0 and 1 (with a control volume measured along a pipe wall and the effect of the boss section considered to be negligible).

$$\Delta E_b = \Delta E_f + \omega r_{1s} (-F_\theta) \quad (F_\theta < 0) \dots\dots\dots (12)$$

Where  $F_\theta$  is the total shear force that will be applied to the fluid from the wall of the suction pipe between positions 0 and 1. Equation (12) shows that the fluid flowing upstream from the impeller transfers angular momentum to the fluid flowing into the impeller (induces positive pre-swirl) through friction force.

Next, the increase in total enthalpy between positions 0 and 2 is studied. The enthalpy of an ideal gas can be obtained by the product of constant pressure specific heat and absolute temperature. The enthalpy of the fluid flowing upstream from the impeller ( $C_p T_{0b}$ ) is assumed as follows:

$$C_p T_{0b} = C_p T_{01} + \beta (u_2 C_{u2} - \Delta E_f / m) \dots\dots\dots (13)$$

In equation (13), the work that the fluid flowing upstream from the impeller obtains in the impeller is assumed to be  $\beta$  times the total enthalpy that the fluid flowing out of the impeller obtains (expressed by the formula in parentheses in the second term on the right-hand side of the equation).

Then, the total enthalpy of the fluid flowing into the impeller at position 1 ( $C_p T_{01}$ ) is:

$$(m_b + m) C_p T_{01} = m_b C_p T_{0b} + m C_p T_0 \dots\dots\dots (14)$$

Using equation (13), equation (14) can be expressed as follows:

$$C_p T_{01} = C_p T_0 + \beta m_b / m (u_2 C_{u2} - \Delta E_f / m) \dots\dots\dots (15)$$

The total enthalpy that the fluid flowing into position 0 (the inlet of the compressor) obtains by flowing through position 2 (the outlet of the impeller) ( $\Delta h_{0-2}$ ) is:

$$\Delta h_{0-2} = C_p T_{02} - C_p T_0 = (1 + \beta m_b / m) (u_2 C_{u2} - \Delta E_f / m) \dots\dots\dots (16)$$

The product of the total enthalpy  $\Delta h_{0-2}$  and the compressor efficiency  $\eta$  is the enthalpy contributing to a pressure increase. The relationship between the compressor efficiency and the pressure ratio can be expressed by:

$$\pi = \left[ 1 + (\eta \Delta h_{0-2}) / (C_p T_0) \right]^{\gamma / (\gamma - 1)} \dots\dots\dots (17)$$

Inlet recirculation grows upstream from the impeller as the

flow rate is reduced. The growth of inlet recirculation is associated with the increases in  $\beta m_b/m$  and  $\Delta E_f/m$ . The increase in  $\Delta E_f/m$  causes a reduction in the work transferred from the impeller to the fluid and has the possibility to generate a positive gradient in the compressor characteristics (the reduction in the pressure ratio due to the reduction in the flow rate). That is, there is a possibility of reducing the surge flow rate by controlling the growth of the pre-swirl due to the inlet recirculation. Also, it can be said that the work supplied from the impeller to the fluid can be considerably increased by controlling the pre-swirl without reducing  $m_b$ .

The following section explains the effects of inlet fins installed in the suction pipe on curbing the growth of inlet recirculation.

#### 4. Characteristics of the tested compressor

**Table 1** shows the major impeller parameters of the turbocharger centrifugal compressor considered in this paper. The radius of the impeller outlet ( $r_2$ ) is 25.5 mm and the number of blades is 12 (6 full blades and 6 splitter blades).

**Figure 4** shows the characteristics of the compressor. The generation of surge was determined by the signals of a high responsive pressure sensor installed at the inlet of the compressor and abnormal sound. The purpose of this research is to reduce the surge flow rate when the peripheral Mach numbers  $Mu$  (equivalent to rotation speeds) are 0.82 and 1.01 without reducing the maximum flow rate when  $Mu$  is 1.50. **Figure 5** shows the static pressure characteristics near the leading and trailing edges of the impeller when  $Mu$  is 0.82 and 1.01. The  $L$  in the figure means the height of the full

**Table 1** Main impeller parameters of automotive turbocharger compressor

Symbol	$r_{1s}/r_2$	$r_{1h}/r_{1s}$	$b_2/r_2$	$\beta_{b1s}$	$\beta_{b2}$
Specification	0.77	0.29	0.13	61°	43°

(Note)  $r_{1s}$ : Shroud radius of impeller inlet  
 $r_{1h}$ : Hub radius of impeller inlet  
 $r_2$ : Radius of impeller outlet  
 $b_2$ : Blade height of impeller outlet  
 $\beta_{b1s}$ : Shroud blade angle of impeller inlet  
 $\beta_{b2}$ : Blade angle of impeller outlet

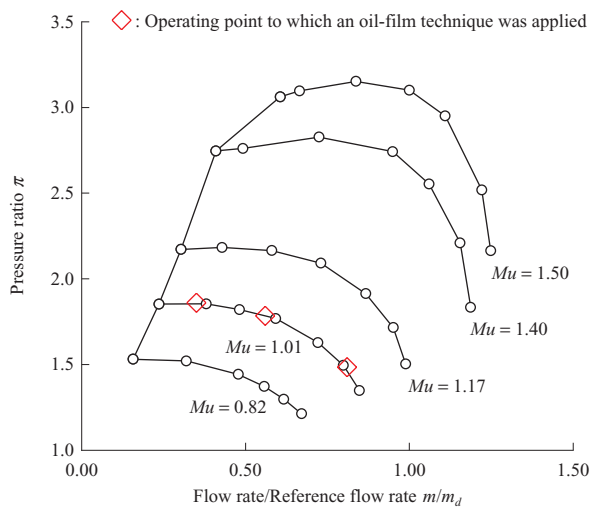
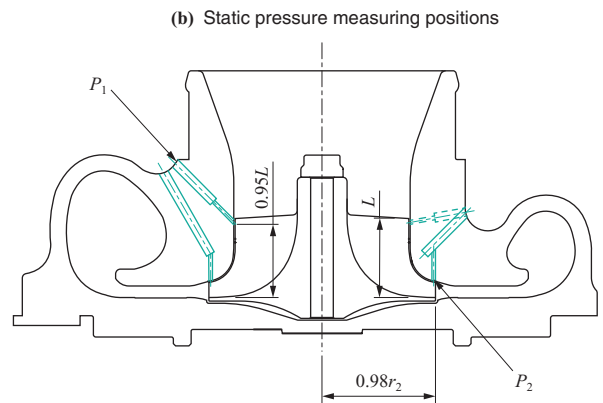
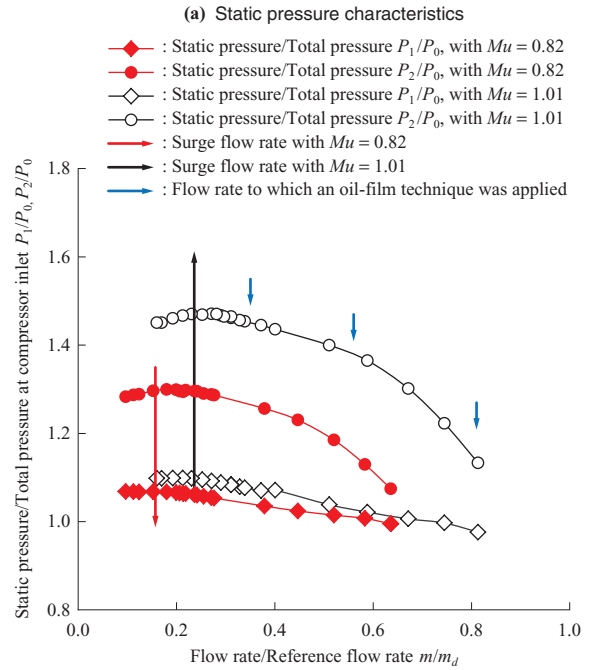


**Fig. 4** Compressor characteristics



(Note)  $L$ : Blade height  
 $r_2$ : Impeller radius  
 $P_1$ : Static pressure (near the leading edge of the impeller)  
 $P_2$ : Static pressure (near the trailing edge of the impeller)

**Fig. 5** Static pressure characteristics at impeller inlet and exit

blades. The data in **Fig. 5** includes the data on flow rates lower than the surge flow rate indicated in **Fig. 4**. These data were obtained by adding an orifice plate to the inside of the exit pipe of the compressor to maintain stable operation of the compressor with a flow rate not more than the surge flow rate of the compressor. The increase in static pressure associated with the reduction in the flow rate near the leading and trailing edges of the impeller saturated at around the surge flow rate.

**Figure 6** shows visualized flows by an oil-film technique when  $Mu$  was 1.01. When  $m/m_d$  was 0.81 (**Fig. 6-(a)**), a straight oil film pattern extended in the pipe axis direction can be seen on the inner pipe wall up to the leading edge section of the impeller. In contrast, when  $m/m_d$  was 0.55 (**Fig. 6-(b)**) close to the maximum efficiency point and 0.35 (**Fig. 6-(c)**) close to the surge point, spiral oil film patterns due to the generation of inlet recirculation can be observed.

The temperatures of the points close to the pipe walls were

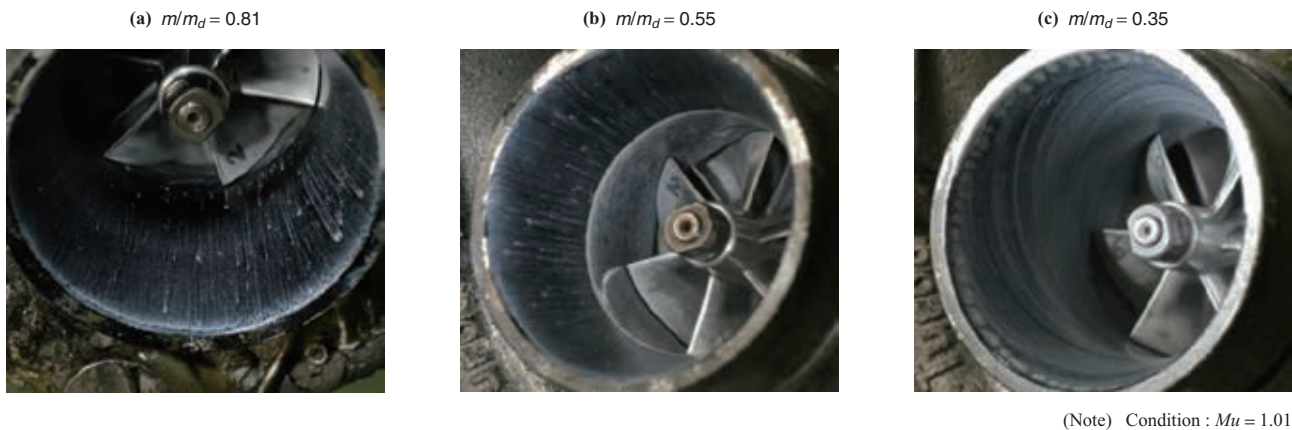


Fig. 6 Result of oil flow visualization<sup>(7)</sup>

measured by inserting thermocouples at several locations along the suction pipe and the measurement results (temperature distribution in the axial direction) are shown in Fig. 7. It can be seen that the temperature was increased due to the growth of a reverse flow region as the flow rate was reduced. Regardless of the values of  $Mu$ , the reverse flow region did not reach the inlet edge of the pipe.

Figure 8 shows visualized flows in the suction pipe by PIV (Particle Image Velocimetry). The operating points of the compressor where PIV measurement was conducted are shown in Fig. 8-(a). In this test, because an acrylic suction pipe was used in the test,  $Mu = 0.58$  was selected as the test condition from the viewpoint of heat resistance. Operating points A to D in Fig. 8 are the same as those in Fig. 7-(a) when  $Mu$  was 0.58. The incidence angles of the impeller shroud which were predicted in the 1-D calculation are also shown in Fig. 8-(a). The measured (visualized) cross sections and regions are shown in Fig. 8-(b). In this test, visualization of flows was conducted for two cross sections, one is the cross section in the pipe axial direction (between the position 3.12 times the impeller tip diameter upstream from the leading edge of the impeller to the trailing edge of the suction pipe) and the other is the cross section in a direction perpendicular to the pipe axis (at the position 1.05 times the tip diameter of the impeller upstream from the impeller). Figure 8-(c) shows the measurement results of speed distribution at the central cross section along the pipe axis. The distribution at measurement points A and B indicates that these points were filled with fluid flowing from upstream to downstream. In contrast, the distribution at measurement points C and D shows reverse flow regions near the pipe wall and expansion of the regions as the flow rate was reduced from C to D. Figure 8-(d) shows the distribution of (circumferential) speed in the pipe cross section. As can be seen in C and D, a swirl flow was generated near the pipe wall. There existed a flow flowing upstream in the suction pipe, i.e. inlet recirculation, in a region near the pipe wall. Also, the flow speed in the pipe axis direction toward the impeller was increased due to the reduction in the effective area caused by the generation of a reverse flow region. Figure 8-(e) shows the measurement result in the surge condition.  $T$  indicates a

surge cycle and surge periods 0.2 to 0.24 s were measured in the test. Different from C and D in Fig. 8-(d), a region with a flow speed of almost 0 can be found in the upstream region of the impeller in Fig. 8-(e).

A turbocharger compressor is designed to maximize the choke flow rate with an impeller having a small diameter. The impeller under test was designed to have an incidence angle of +3 degrees with a choke flow rate when  $Mu$  was 1.50. Therefore, the incidence angle at the maximum efficiency point ( $m/m_d = 0.55$ ) was 12 degrees when  $Mu$  was 1.01. Thus, a turbocharger compressor is likely to generate inlet recirculation in a low rotation speed region and it is difficult to reduce its surge flow rate.

## 5. Performance of the compressor with inlet fins

Figure 9 shows the installation state of inlet fins. These inlet fins were installed on an inner circumference 53 mm upstream from the leading edge of the impeller and directed parallel to the pipe axis and the flow direction in the pipe. These fins had an inclination angle of 20 degrees in the direction opposite to the rotational direction of the impeller when viewed from the front of the suction pipe. Although other sets of inlet fins with inclination angles of 0 and 20 degrees in the rotational direction of the impeller were also tested, there were no differences in the test results. In order to avoid the reduction in the choke flow rate when  $Mu$  was 1.50, the inner diameter of the inlet fins was designed to be equal to the diameter of the impeller inlet.

Figure 10 shows the results of comparison of the compressor characteristics with and without the inlet fins and Fig. 11 shows the comparison of the compressor efficiencies with and without the inlet fins when  $Mu$  was 0.82, 1.01 and 1.50. Table 2 shows the surge improvement rate  $\Delta m_s$ , defined by the formula in the table. Here, the surge flow rate is the minimum flow rate allowing the compressor to operate stably. In the test, the surge flow rates when  $Mu$  was 0.82 and 1.01 were successfully reduced while maintaining the maximum flow rate when  $Mu$  was 1.50. Also, stabilization of the compressor characteristic was achieved with a negative gradient of the characteristic curve in the region near the surge when  $Mu$  was

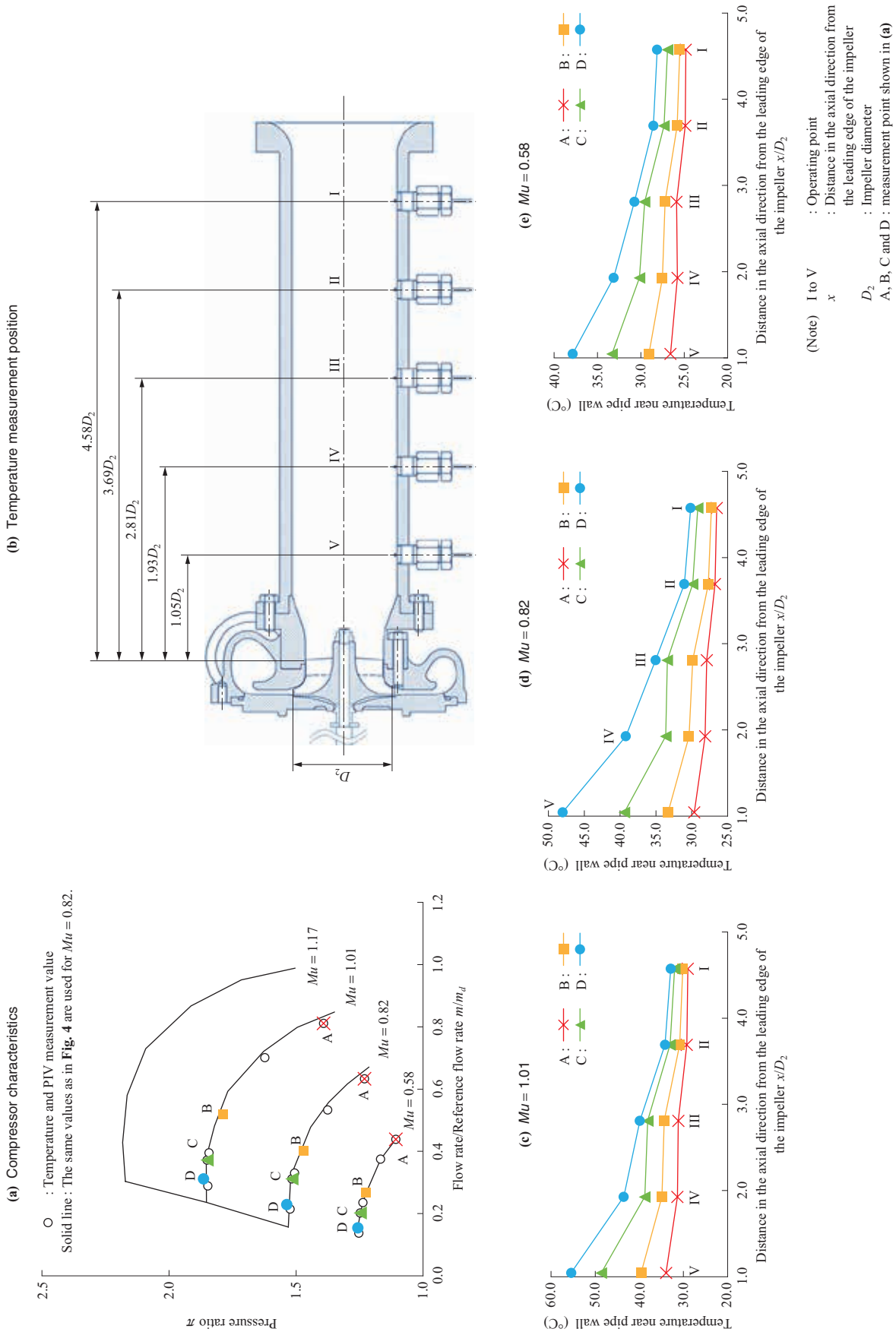
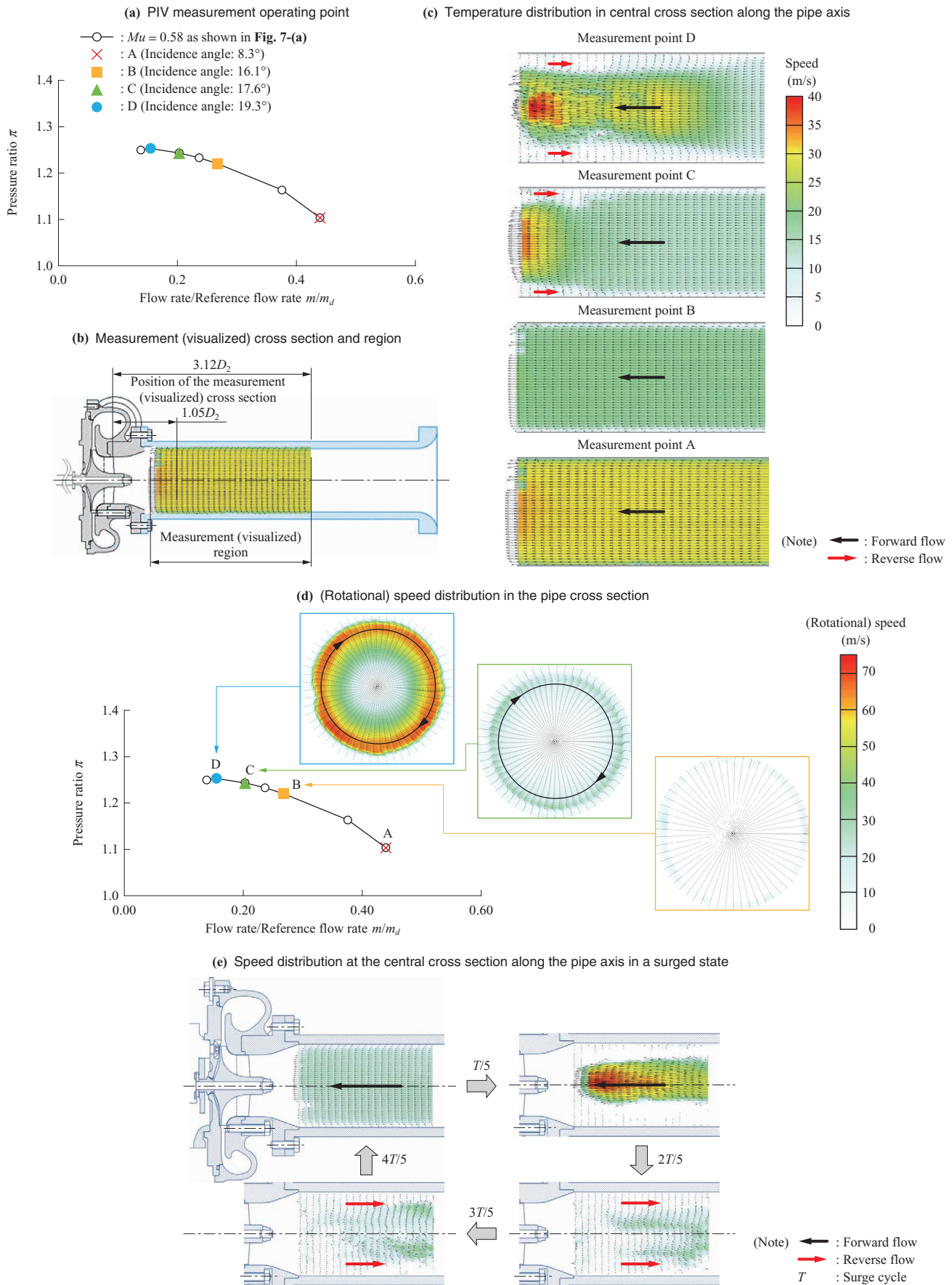


Fig. 7 Temperature distribution along suction pipe



**Fig. 8 Results of flow visualization with PIV**

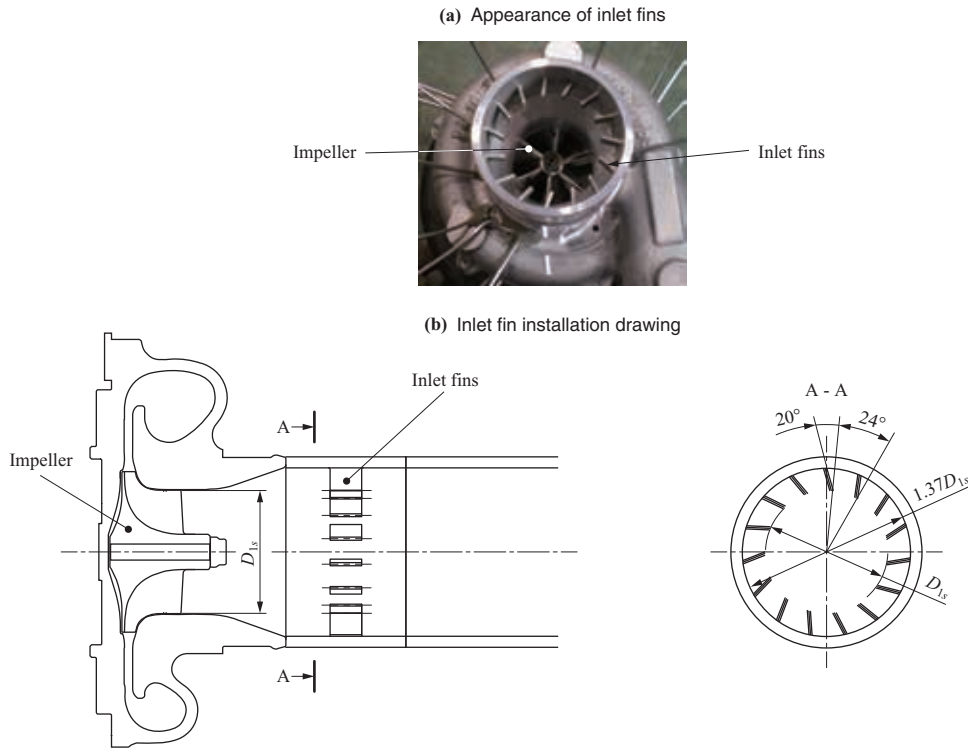


Fig. 9 Tested inlet fins<sup>(7)</sup>

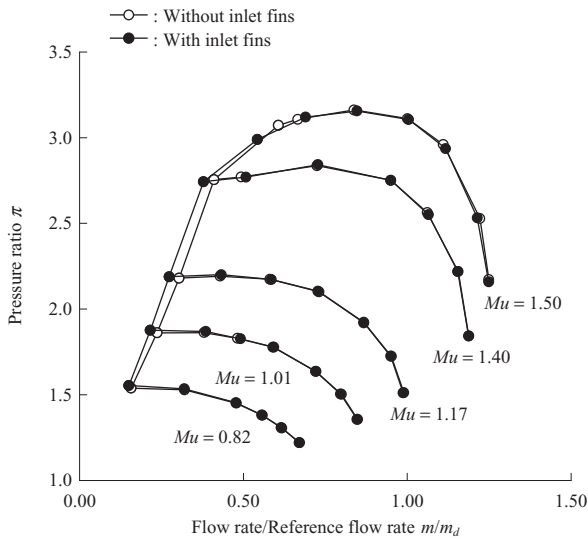


Fig. 10 Comparison of compressor characteristics with and without inlet fins

0.82 and 1.01. No reduction in compressor efficiency was found except in the region near the surge flow rate. As mentioned in the following section, the reduction in compressor efficiency indicates that inlet recirculation reached the position of the inlet fins.

Figure 12 shows a comparison of the static pressure at the areas close to the leading and trailing edges of the impeller with and without the inlet fins. The data in Fig. 5 are also shown in Fig. 12 for comparison. As shown in Fig. 12, the installation of the inlet fins enabled the pressure characteristics at the leading edge and outlet of the impeller to have a negative gradient and the compressor characteristics to be

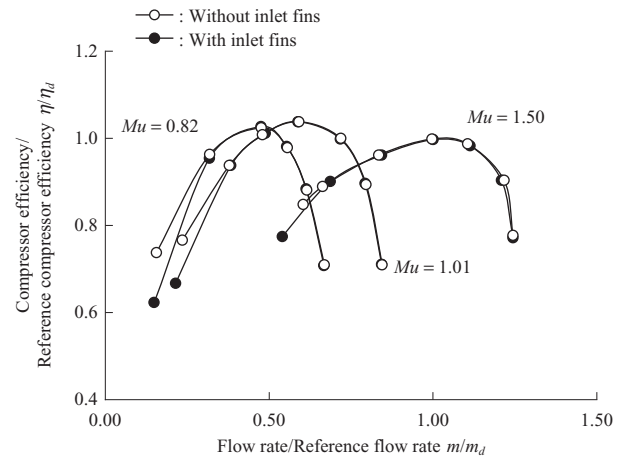


Fig. 11 Comparison of compressor efficiency with and without inlet fins

Table 2 Surge improvement rate due to use of inlet fins

$Mu$ (-)	$\Delta m_s$ (%)	Formula for calculating surge improvement rate
0.82	4.6	$\Delta m_s = \left( 1 - \frac{\text{Surge flow rate with inlet fins}}{\text{Surge flow rate without inlet fins}} \right) \times 100 \text{ (\%)}$
1.01	9.8	
1.17	11.0	
1.40	8.5	

(Note)  $Mu$  : Circumferential speed Mach number  
 $\Delta m_s$  : Surge improvement rate

stabilized. The inlet fins also contributed to moving the local maximum point of the static pressure toward the side with the lower flow rate.

Flow analysis using CFD was conducted to investigate the

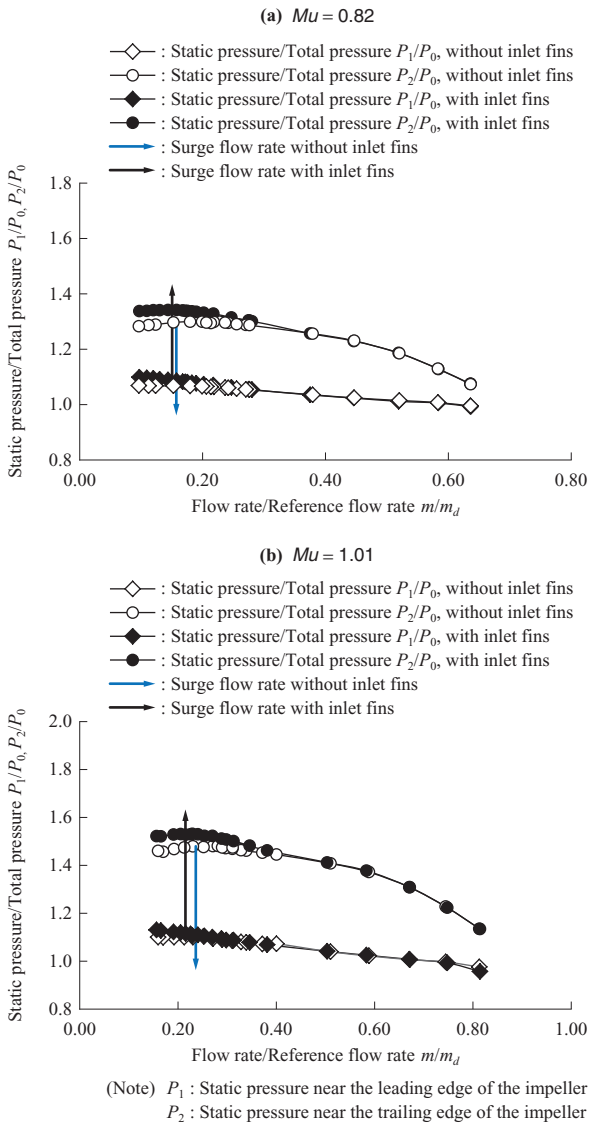


**Fig. 12** Comparison of static pressure at impeller inlet and exit with and without inlet fins

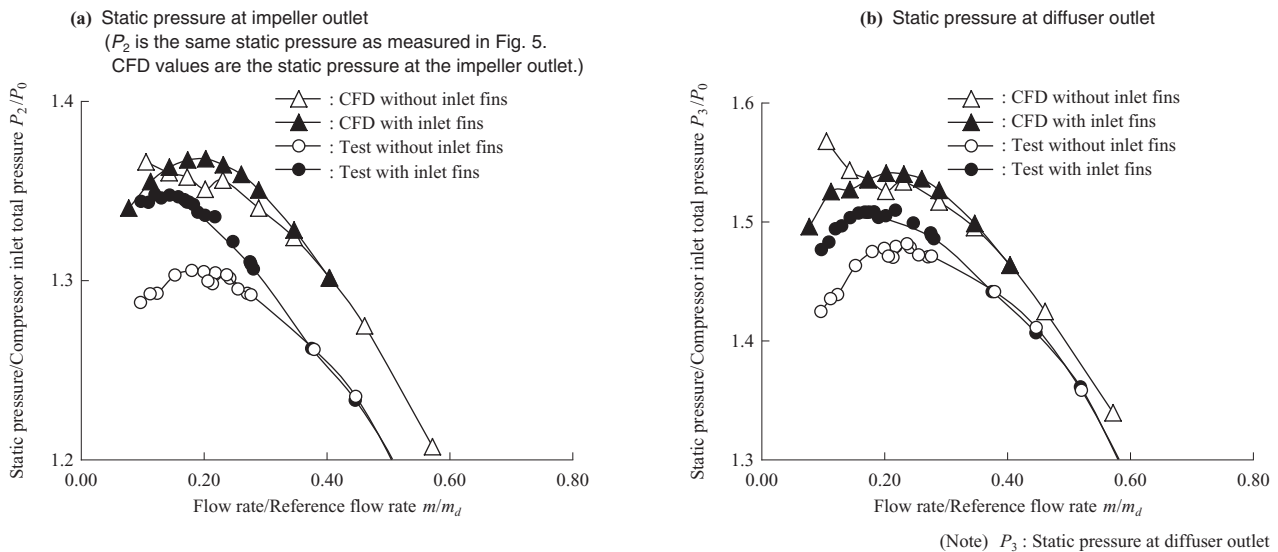


**Fig. 13** Results of static pressure measurement and calculations (CFD)

difference in the flow fields with and without the inlet fins. In the analysis, calculations were based on original code developed by IHI using the RANS (Reynolds-Averaged Navier-Stokes) model. In addition, the single pitch models of an inlet fin and an impeller blade were established with a mixing plane in between. The analysis did not include a volute. The TVD (Total Variation Diminishing) scheme by Chakravarthy-Osher was used for the convection term and the Spalart-Allmaras model was used for the turbulence model. The analysis used about 5.5 million grid points to investigate the difference in the flow fields with and without the inlet fins including 21 grid points in the space between the blade tips formed by the impeller and the casing. The dimensionless distance from wall  $y^+$  was kept below 3. The inlet boundary was arranged at a sufficiently upstream position to avoid its influence on inlet recirculation. The analysis was conducted with  $Mu$  set at 0.82. Because inlet recirculation is associated with swirls having a very unsteady nature, steady analysis using a mixing plane was considered to be inappropriate for quantitative evaluation. Thus, this paper addresses the qualitative evaluation of the effects of the inlet fins on a flow and the validation of the previous discussion on inlet recirculation using a 1-D model.

**Figure 13** shows a comparison of the results of the static pressure measurement at the impeller and diffuser outlets with the calculation results (CFD). Here,  $P_2$  is the same static pressure as measured in **Fig. 5**. The CFD values are the static pressure at the impeller outlet. The calculation and measurement results show a similar tendency until  $m/m_d$  reached 0.20 with a local maximum value of the pressure shifted to the side of a lower flow rate as an effect of the inlet fins. First, the flow field when  $m/m_d$  was 0.20 is discussed below.

**Figure 14** shows the spanwise distributions of speeds in the axial and circumferential directions at the leading edge of the impeller. The circumferentially averaged speeds were used in both distributions. In the figure, negative speeds mean that

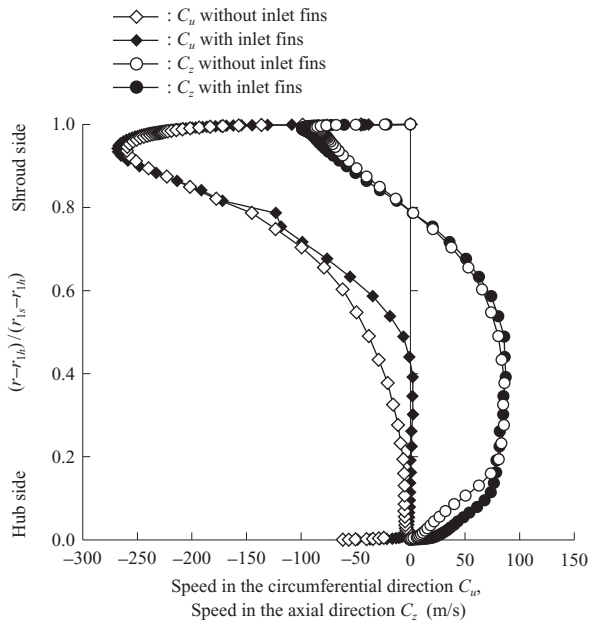


**Fig. 14** Axial and circumferential velocity distribution at impeller leading edge at  $m/m_d = 0.2$

the speed component in the circumferential direction was equal to the rotational direction of the impeller (positive pre-swirl).

**Figure 15** shows the distribution of the total pressure (averages in the circumferential direction) in a span direction at the leading edge of the impeller. The flow flowing upstream of the impeller existed in a region corresponding to 20% of the span from the shroud. The increases in the total pressure were concentrated in this region. The inlet fins reduced the positive pre-swirl (negative speed in the circumferential direction in the figure) of the fluid recirculated into the impeller in the range with  $C_z > 0$ . That is, the inlet fins increased the work transferred from the impeller to the fluid ( $(m u_2 C_{u2} - \Delta E_f)$  in equation (11)).

**Figure 16** shows the streamlines and the distribution of the

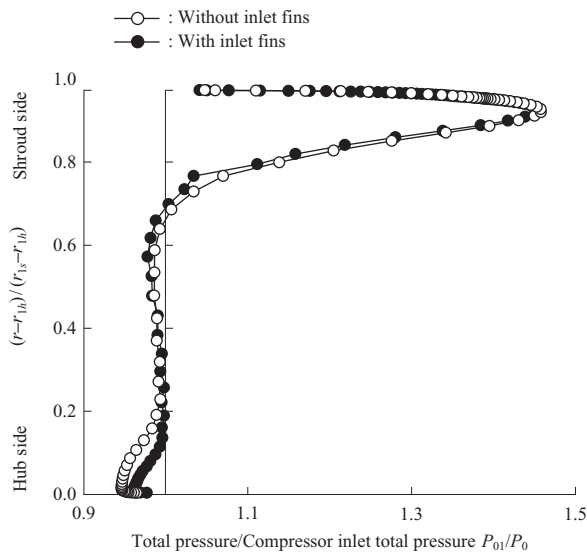


**Fig. 15** Total pressure distribution at impeller leading edge

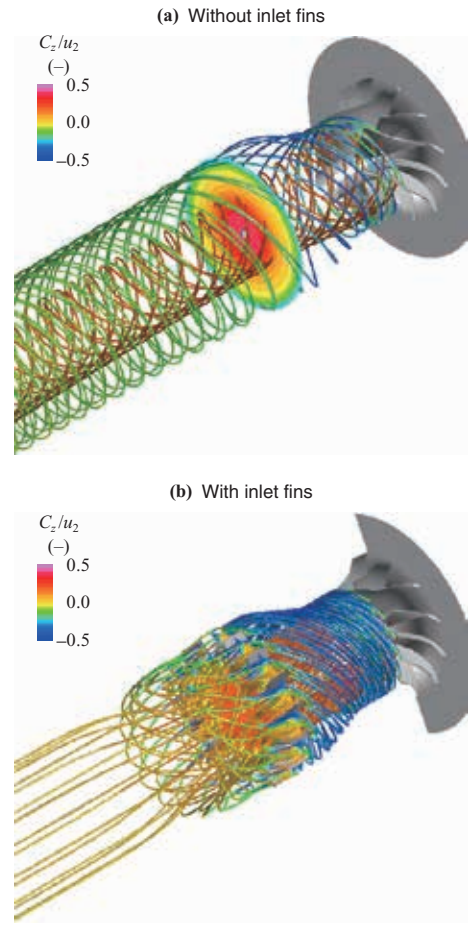


**Fig. 16** Streamline and axial velocity distribution at  $m/m_d = 0.20$

speeds in the axial direction when  $m/m_d$  was 0.20. The contour plot in **Fig. 16-(a)** corresponds to the installation position of the inlet fins. The colors of the contour lines and streamlines indicate magnitudes of the speed in the axial direction. When the flow flowing upstream from the impeller reached the inlet fins, the flow interfered with the inlet fins and lost its swirling speed components. The swirling speed components caused a pressure difference that induced a reverse flow upstream of the suction pipe. Thus, the flow flowing upstream through the inlet fins from the downstream side of the suction pipe could not flow further upstream due to the inlet fins' effect of preventing inlet recirculation from spreading upstream. The inlet fins prevented the exchange of the angular momentum from the flow flowing out of the impeller to the flow flowing into the impeller, thereby weakening positive pre-swirl at the inlet of the impeller.

**Figure 17** shows the streamlines and the distribution of the speeds in the axial direction when  $m/m_d$  was 0.35. As can be seen, the region where inlet recirculation existed and the strength of swirling were less than those when  $m/m_d$  was 0.20. **Figure 18** shows the distributions of the speeds in the axial direction and circumferential direction ( $m/m_d = 0.35$ ). The averages in the circumferential direction were used in both distributions. No change was produced in the distribution of the speeds regardless of the presence of the inlet fins. One possible reason for that is that the inlet recirculation was too

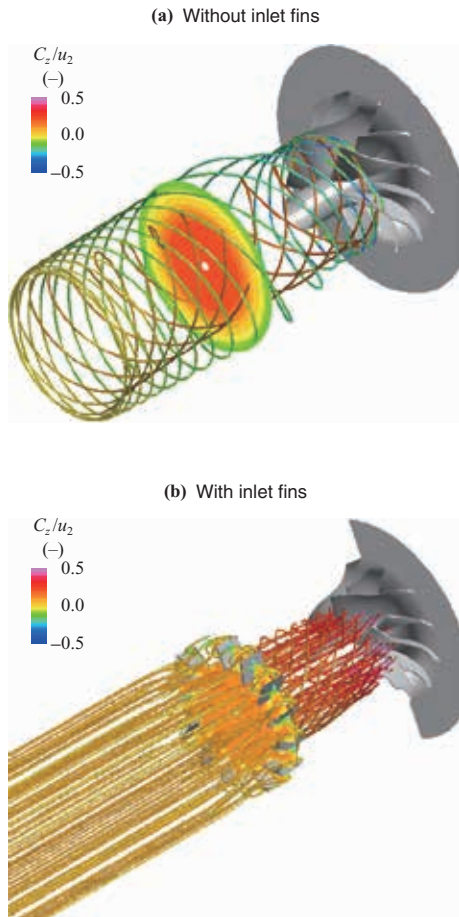


Fig. 17 Streamline and axial velocity distribution at  $m/m_d = 0.35$

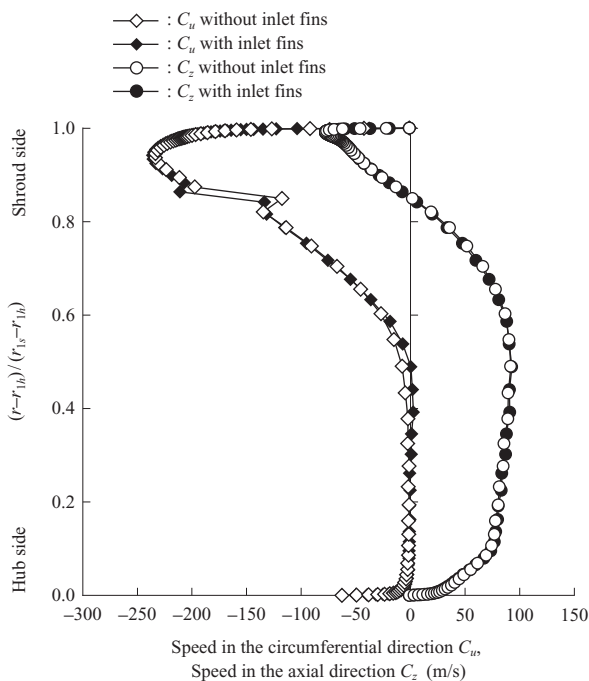


Fig. 18 Axial and circumferential velocity distribution at impeller leading edge at  $m/m_d = 0.35$

weak to reach the inlet fins. The inlet fins only work when the inlet recirculation reaches them.

Thus, it is clear that the installation position of the inlet fins is an important parameter.

Figure 19 shows (the calculation results of) the impeller efficiencies. The impeller efficiency gradually declined as  $m/m_d$  was reduced from 0.35. One of the reasons for the decline in the impeller efficiency is that the installation of the inlet fins caused a reduction in the positive pre-swirl and an increase in the incidence angle of the flow flowing into the impeller. Figure 20 shows the distributions of the relative

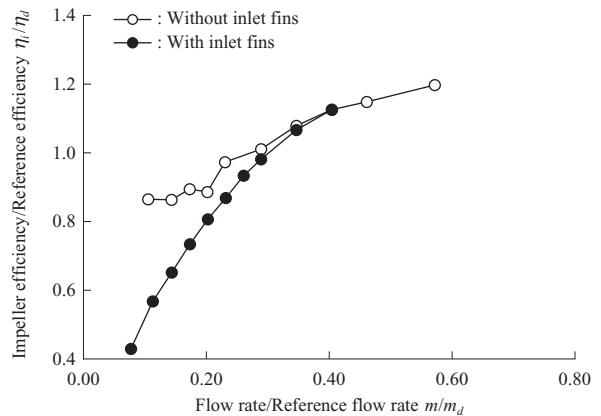


Fig. 19 Impeller efficiency obtained with CFD (calculation results)

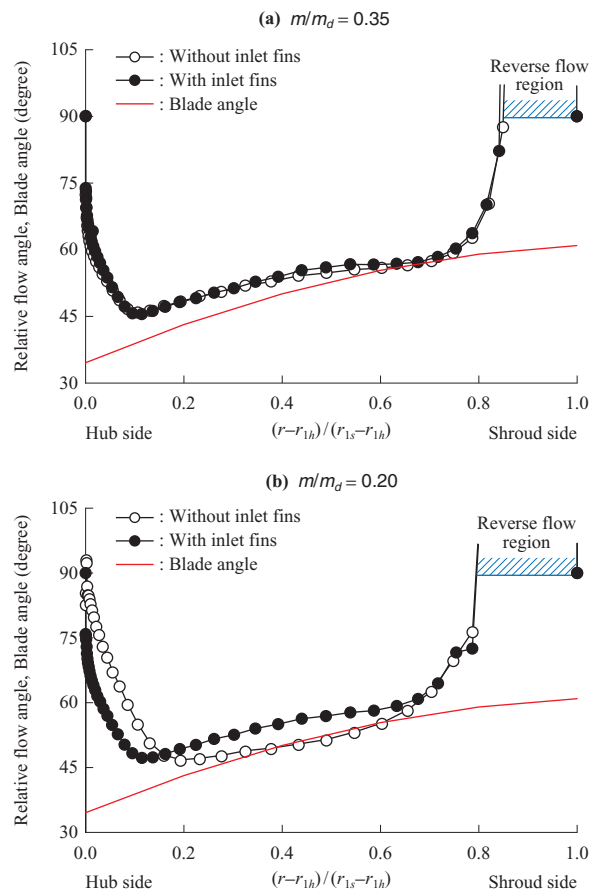


Fig. 20 Relative flow angle and blade angle distribution at impeller leading edge

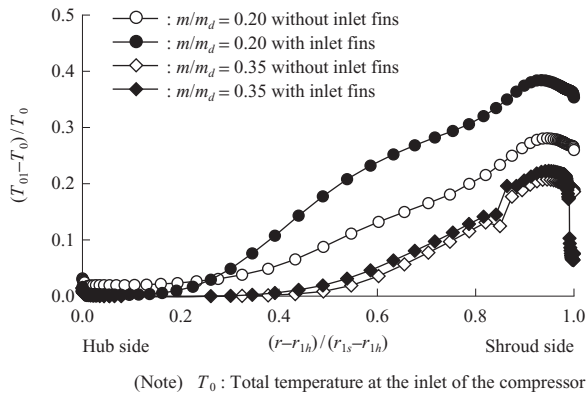


Fig. 21 Total temperature distribution at impeller leading edge

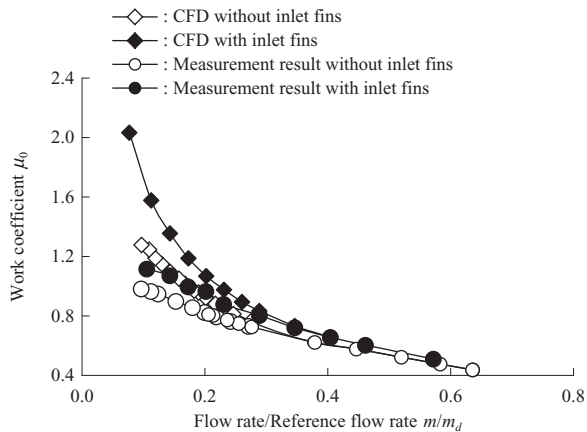


Fig. 22 Work coefficient

flow angles and blade angles at the leading edge of the impeller. The averages in the circumferential direction at respective span positions were used in both distributions. Without inlet fins, the difference between the relative flow angle and the impeller blade angle (incidence angle) was reduced when  $m/m_d$  was reduced from 0.35 to 0.20. In contrast, with the inlet fins, the reduction in  $m/m_d$  from 0.35 to 0.20 caused an increase in the difference between the relative flow angle and the impeller blade angle (incidence angle).

Figure 21 shows the distribution of the total temperature at the leading edge of the impeller. The averages in the circumferential direction at each span position were used. In the figure,  $T_0$  means 293 K. Figure 22 shows the work coefficients obtained through the test and analysis. As predicted with the 1-D model, the installation of the inlet fins caused increases in the temperature at the inlet of the impeller and the work coefficient. In the case of a turbocharger, an increase in the work coefficient means an increase in turbine power to drive a compressor.

## 6. Conclusion

- (1) The effects of inlet recirculation on compressor

characteristics were discussed using a 1-D model. The discussion showed that the growth of inlet recirculation associated with a reduction in the flow rate may cause the compressor characteristics to have a positive gradient, thereby destabilizing the operation of the compressor.

- (2) The installation of the inlet fins controls the growth of pre-swirl, which is the main factor that allows inlet recirculation to cause the compressor characteristics to have a positive gradient, enabling the surge flow rate to be reduced in a low rotation speed region. Controlling pre-swirl causes a reduction in the compressor efficiency when the flow rate is close to the surge flow rate and, therefore, the trade-off between efficiency and operating range is required.
- (3) The installation of the inlet fins increases the work coefficient. In the case of a turbocharger, an increase in the work coefficient means an increase in the turbine power to drive a compressor. Thus, the trade-off between the operating range and turbocharger response is required.
- (4) The inlet fins are an effective means of preventing inlet recirculation from growing upstream from the impeller.

## REFERENCES

- (1) Y. Hirai : Recent IHI Turbocharger Technologies for Automotive Engines Turbomachinery Vol. 43 No. 9 (2014. 9) pp. 26-33
- (2) P. Harley, S. Spence and J. Early : Inlet Recirculation in Automotive Turbocharger Centrifugal Compressors 11th International Conference on Turbochargers and Turbocharging (2014. 5) pp. 89-100
- (3) H. Tamaki : Study on Flow Fields in Centrifugal Compressor with Unpinched Vaneless Diffuser IHI Engineering Review Vol. 48 No. 2 (2015. 12) pp. 15-24
- (4) P. Harley, S. Spence, D. Filsinger, M. Dietrich and J. Early : Meanline Modelling of Inlet Recirculation in Automotive Turbocharger Centrifugal Compressors Journal of Turbomachinery Vol. 137 No. 1 (2014. 9) pp. 011 007-1-011 007-9
- (5) X. Qui, D. Japikse and M. Andersen : A Meanline Model for Impeller Recirculation Proceedings of ASME TURBO EXPO GT2008-51349 (2008. 7) pp. 1-8
- (6) J. Andersen, F. Lindström and F. Westin : Surge Definitions for Radial Compressors in Automotive Turbochargers SAE Technical Paper 2008-01-0296 (2008. 4) pp. 1-14
- (7) H. Tamaki, M. Unno, R. Tanaka, S. Yamaguchi and Y. Ishizu : Enhancement of Centerifugal Compressor Operating Range by Control of Inlet Recirculation with Inlet Fins Proceedings of ASME TURBO EXPO GT2015-42154 (2015. 1) pp. 1-12